

Quantum Energy Border in Vibrational Spectra of Polynomial Molecular Potentials

Alessio Del Monte

Dipartimento di Fisica, Università degli Studi di Milano, Via Celoria 16, I-20133 Milano

Nicola Manini*

*Dipartimento di Fisica, Università degli Studi di Milano, Via Celoria 16, I-20133 Milano and
INFM, Unità di Milano, Milano, Italy*

Luca Molinari†

*Dipartimento di Fisica, Università degli Studi di Milano and INFN,
Sezione di Milano, Via Celoria 16, I-20133 Milano*

Gian Paolo Brivio‡

*Dipartimento di Scienza dei Materiali, Università di Milano-Bicocca, Via Cozzi 53, I-20125 Milano and
INFM, Unità di Milano-Bicocca, Milano, Italy*

(Dated: October 31, 2003)

Polynomial approximations around the global minimum of the adiabatic potential energy surface of several polyatomic molecules display an unphysical saddle point of comparatively small energy, leading to a region where the potential is negative and unbounded. This poses an energy upper limit for a reliable evaluation of the vibrational levels. We argue that the presence of such saddle points is general. The effect of tunneling through the saddle is explored by means of non-perturbative evaluations of vibrational spectra based on a tier by tier construction of the basis and an exact recursive equation for the resolvent.

PACS numbers: 33.20.Tp, 33.15.Hp, 82.20.Kh

I. INTRODUCTION

The morphology of the adiabatic potential energy surface (APES), especially its low-energy minima and saddle points, is at the basis of the quantum chemistry of reaction paths and conformational transitions.¹ The adiabatic potential governs the low-energy vibrational dynamics of a rigid molecule of N atoms and is a complicate function of $d = 3N - 6$ internal coordinates, such as bond lengths, bending or torsion angles ($d = 3N - 5$ for linear molecules). Its actual determination is usually a very demanding problem,² as the information contents of a function of d coordinates grows exponentially with d . A standard approximate parametrization is provided locally by a Taylor expansion around the global minimum \mathbf{q}^0

$$V^{\text{ad}}(\mathbf{q}) = V^{\text{ad}}(\mathbf{q}^0) + \frac{1}{2} f_{ab}(q_a - q_a^0)(q_b - q_b^0) + V^{\text{anh}}(\mathbf{q} - \mathbf{q}^0). \quad (1)$$

Here, $f_{ab} = \partial^2 V^{\text{ad}} / \partial q_a \partial q_b|_{\mathbf{q}^0}$ is the Hessian matrix and V^{anh} collects all residual higher-order terms. For convenience we take the energy zero such that $V^{\text{ad}}(\mathbf{q}^0) = 0$. For a sharp minimum, the kinetic energy can be separated into the energy of a rigid rotator, a vibrational term, and a mixed Coriolis term that is treated as a perturbation. The simultaneous diagonalization of the Hessian matrix f_{ab} and of the vibrational kinetic quadratic form defines the normal-mode harmonic frequencies ω_a and the dimensionless normal-mode coordinates Q_a measured with respect to the equilibrium geometry.³ In terms

of these, the expansion of the vibrational Hamiltonian becomes:

$$H = \frac{1}{2} \sum_a \hbar \omega_a (P_a^2 + Q_a^2) + \frac{1}{3!} \sum_{abc} \Phi_{abc} Q_a Q_b Q_c + \frac{1}{4!} \sum_{abcd} \Phi_{abcd} Q_a Q_b Q_c Q_d + \dots \quad (2)$$

The frequencies ω_a and higher-order force constants $\Phi_{ab\dots}$ of several molecules have been computed *ab-initio*, and sometimes refined by comparison with spectroscopic data.⁴ For a simple molecule such as water, the force constants have been determined up to sixth order,⁵ and for several polyatomic molecules the literature reports calculations of third and fourth-order force constants.^{6,7,8,9} Hereafter, we shall refer to the (finite) polynomial potential in Eq. (2) as to the PP.

We consider the available data for the PP of several molecules. In all cases we find a saddle point of comparatively small energy, leading to an unphysical dissociative region where the potential is not bounded from below. We also find that, for most molecules, the potential well accommodates very few quantum levels up to the saddle energy. To our surprise, this problem seems to be neglected: its analysis is the main purpose of the present study.

The standard use of the polynomial expansion (2) is the calculation of a number of vibrational levels, usually by means of perturbation or variational theories, or by numerical diagonalization. Contrary to finite-order perturbative calculations, a non-perturbative determination of vibrational levels inevitably detects tunneling to

the unphysical region through the saddle. We show that the presence of this unphysical saddle is a serious issue, affecting radically the range of applicability of exact calculations based on the approximate PP. For this purpose we develop and make use of a non-perturbative technique (equivalent to exact diagonalization on a large basis) that consists in a recursive evaluation of the Green function in a reduced basis obtained by a “tier by tier” construction. The basic outcome of these calculations is that sharp vibrational levels do occur only in the energy region below a quantum energy border, given by the sum of the energy of the lowest saddle (the classical border) plus a quantum correction. The latter is the zero-point energy of the $d-1$ “transverse” modes (of positive curvature) at the saddle point.

The paper is organized as follows: In Sec. II we present the data for the lowest unphysical saddle point of some molecules, based on force constants available in the literature, and give arguments for the general occurrence of a low-energy saddle in polynomial approximations of the molecular APES. The quantum energy border for the tunneling regime is introduced in Sec. III. The influence of the quantum energy border on the stability of vibrational levels is illustrated by applying our non-perturbative method to a simple two-dimensional model. In Sec. IV we apply these concepts to the spectrum of the water molecule, and in Sec. V we discuss the results and the ensuing scenario. The computational method, with the main iterative formula Eq. (A4), is presented in the Appendix.

II. THE UNPHYSICAL SADDLE

A unique feature of the polynomial expansion in Eq. (2) for the special case of diatomic molecules ($d=1$) is that many even-power terms are *positive* (for example *all* even-power terms are positive for the Morse and Lennard-Jones functions). As a consequence, the truncation of the series to a positive even-power coefficient gives a *lower-bounded* potential, and thus a well-defined quantum problem, characterized by an infinite set of discrete levels. In addition, for the Morse potential it occurs that the second-order perturbative levels, based on a fourth-order PP approximation, reproduce the exact Morse levels.¹⁰ These features for $d=1$ are unfortunately lost when the power expansion (2) is extended to polyatomic molecules ($d > 1$): in all systems which we could obtain the anharmonic parameters for, we verified the occurrence of regions where the fourth-order PP is unbounded below.

Energy barriers separate different minima of a *physical* APES, corresponding to different local equilibrium configurations (isomers) of the molecule. The isomerization dynamics occurs mainly *via* quantum tunneling or thermal activation through the lowest saddle of the barrier¹¹. Likewise, for the PP energy barriers separate the region of the physical minimum around which the expansion

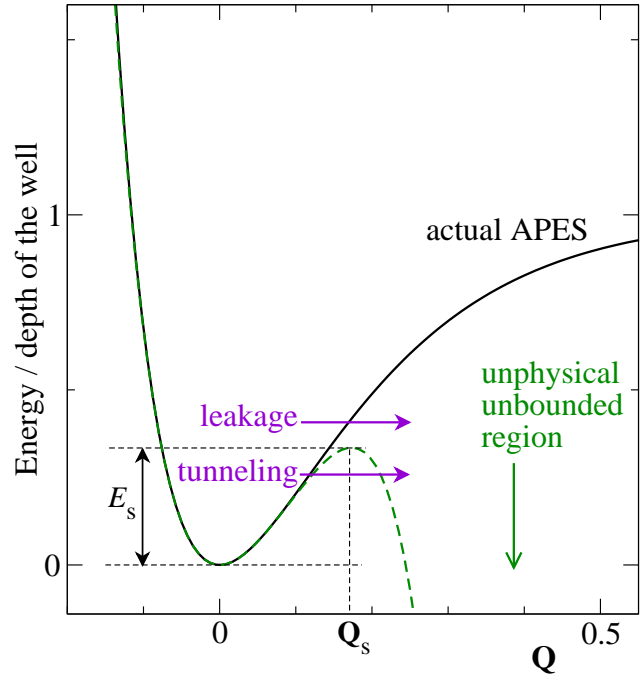


FIG. 1: A typical 1-dimensional molecular potential (Morse, solid) and its 5th-order polynomial approximation (dashed) illustrating the presence of an unbounded region separated from the physical confining region by a barrier topping at a saddle point \mathbf{Q}_s .

is based and well grounded, from the *unphysical* regions where the potential drops to $-\infty$. The escape to the unphysical region is driven by the lowest saddle which introduces an energy “border” that limits the range for (meta-stable) quantum levels allowed in the physical well of the PP. Figure 1 illustrates this concept in a simple $d=1$ -dimensional context, where we purposely truncated the polynomial expansion (2) to an odd order. It is clear that the saddle lies in a region where the polynomial has already become a poor approximation to the actual APES.

To determine the lowest saddle point of the PP of a polyatomic molecule, we first locate all stationary points in the neighborhood of $\mathbf{Q}=\mathbf{0}$ by solving numerically the equation $\nabla_{\mathbf{Q}}V = \mathbf{0}$, and then check that they are indeed saddle points, characterized by one negative and $d-1$ positive curvatures. Finally, for the saddle point \mathbf{Q}_s with lowest energy, we verify that the PP, restricted to the straight line through the points $\mathbf{Q}=\mathbf{0}$ and \mathbf{Q}_s , has a shape qualitatively similar to the dashed line of Fig. 1, i.e. that tunneling indeed occurs through a single barrier to a region where the potential drops to $-\infty$.

Table I reports the height E_s of the lowest (unphysical) saddle point of the PP for several polyatomic molecules, measured from the bottom of the potential well. The values of E_s of different molecules are determined by the characteristic anharmonicities of the molecular bonds and are thus fairly similar, in the 10^3 to 10^4 cm^{-1} range for quartic PP (they are much lower for molecules char-

species	E_s cm^{-1}	$E_{\text{zp}}(\mathbf{0})$ cm^{-1}	E_{zp}^\perp cm^{-1}	Ref.
N_2	18619 [†]	1180	-	12
N_2	32834 [‡]	1180	-	12
HCl	14919 [‡]	1495	-	12
H_2O	6846	4717	4803	5
HOCl	2821	2911	2893	13
$\text{H}_2\text{C}_2\text{O}$	936	7155	6873	14
CH_3OH	50	11398	11276	15

TABLE I: Lowest saddle-point energy E_s , harmonic zero-point energy at the minimum $E_{\text{zp}}(\mathbf{0})$, harmonic transverse zero-point energy at the saddle point E_{zp}^\perp , of the 4th-order PP of several polyatomic molecules ([†]3rd or [‡]5th-order expansion of Morse potential for diatomics). Energies are expressed in spectroscopical wavenumber units cm^{-1} .

acterized by soft torsional modes, such as methylene (CH_3OH). Surprisingly, these saddles are low: about few times a typical harmonic vibrational frequency of the molecule. As a result, only few, if any, vibrational states sit below E_s . This is especially true for molecules with a large number of atoms, where the ground-state energy lies substantially above the bottom of the well, by an amount proportional to d , that easily compares or exceeds the saddle energy E_s .

The occurrence of a saddle leading to an unphysical region is by no means specific of the PP of the molecules listed in Table I: we argue that this is a general feature to be found in the PP of most polyatomic molecules. Indeed, also for an even-power truncation, the PP can easily drop to $-\infty$ in some direction in \mathbf{Q} space³⁶. The precise value of the 4th-order parameters Φ_{abcd} (including their sign) is determined by the *local* properties of the physical APES at its minimum $\mathbf{Q} = \mathbf{0}$, not by any requirement of confining behavior at large distance: the PP of a real molecule easily contains negative semi-diagonal terms Φ_{aabb} and sizable mixed terms Φ_{abcd} , which in turn produce regions where the PP drops to $-\infty$. In practice, the same argument prevents confining behavior also of 6th and higher even-order terms, and an even-power truncated PP does not behave any better, away from the physical minimum, than an odd-power truncated PP. Therefore, we consider it extremely unlikely (though technically possible) that a real polyatomic molecular potential may ever be found whose polynomial expansion at the minimum (truncated at any order > 2) is lower-bounded everywhere.

III. THE QUANTUM ENERGY BORDER

As the PP has no lower bound, the associated Schrödinger problem is ill-defined. However, resonant states with complex energy values $E_a - i\Gamma_a$ usually exist in the well. The imaginary part is proportional to the

inverse lifetime of the state, and it is easily seen to be also proportional to the tunneling current through the barrier. Γ_a can be evaluated by semiclassical methods, like WKB or instanton approach^{16,17,18}, or by complex dilatation^{19,20,21}. Deep in the well, Γ_a is in general exponentially small and proportional to the Gamow factor $e^{-2S/\hbar}$, where S is the imaginary-time action along the most probable tunneling path inside the barrier. Resonances appear as sharp peaks in the spectral density, at energies E_a extremely close to the eigenenergies of the Schrödinger equation restricted to the well. As energy increases toward the threshold value, tunneling evolves into a “leaking” regime, characterized by the appearance of resonances whose imaginary part Γ_a is comparable to the real part¹⁹, relics of further excited states in the well, strongly hybridized to the continuum. In one dimension, the threshold energy coincides with the saddle one E_s .

For $d > 1$, an effect absent in the simple one-dimensional picture of Fig. 1 is to be considered: tunneling through the barrier at the saddle point is hindered by the “transverse” motion of the degrees of freedom perpendicular to the one crossing the barrier. These perpendicular degrees of freedom are associated to a minimum energy E_{zp}^\perp due to Heisenberg’s uncertainty, that adds to the saddle height to determine the quantum energy border between the tunneling and the leaking regimes

$$E_{\text{qb}} = E_s + E_{\text{zp}}^\perp. \quad (3)$$

As the study of tunneling problems^{15,22} suggests, we approximate E_{zp}^\perp by its harmonic expression

$$E_{\text{zp}}^\perp \simeq \frac{1}{2} \sum_{i=2}^d \hbar \omega'_i \quad (4)$$

in terms of the $d - 1$ real harmonic frequencies ω'_i at the saddle point (ω'_1 is the imaginary frequency associated to the tunneling direction). Since, for most polyatomic molecules, E_{zp}^\perp is close to the zero-point energy of the ground state $E_{\text{zp}}(\mathbf{0})$ (see Table I), the raising of the energy border due to E_{zp}^\perp recovers a spectral range ($E_{\text{zp}}(\mathbf{0}) \lesssim E \lesssim E_{\text{qb}}$) where quasistationary vibrational levels are to be found, of extension comparable to the classical region for bounded motion ($0 \leq E \leq E_s$).

To illustrate the quantum energy border, we propose and discuss the following two-dimensional model Hamiltonian

$$\begin{aligned} H &= \frac{\hbar \omega_x p_x^2 + \hbar \omega_y p_y^2}{2} + U(x, y) \quad (5) \\ U(x, y) &= \frac{\hbar \omega_x x^2 + \hbar \omega_y y^2}{2} - \frac{(\hbar \omega_x)^{3/2}}{3\sqrt{6E_s}} x^3 \\ &\quad + \hbar \frac{\omega_s^2 - \omega_y^2}{\omega_y} \left[\frac{\hbar \omega_x}{4E_s} - \left(\frac{\hbar \omega_x}{6E_s} \right)^{3/2} x \right] x^2 y^2, \end{aligned}$$

where the vibrational coordinates x and y are dimensionless, like Q_a in Eq. (2). This potential is simple enough to

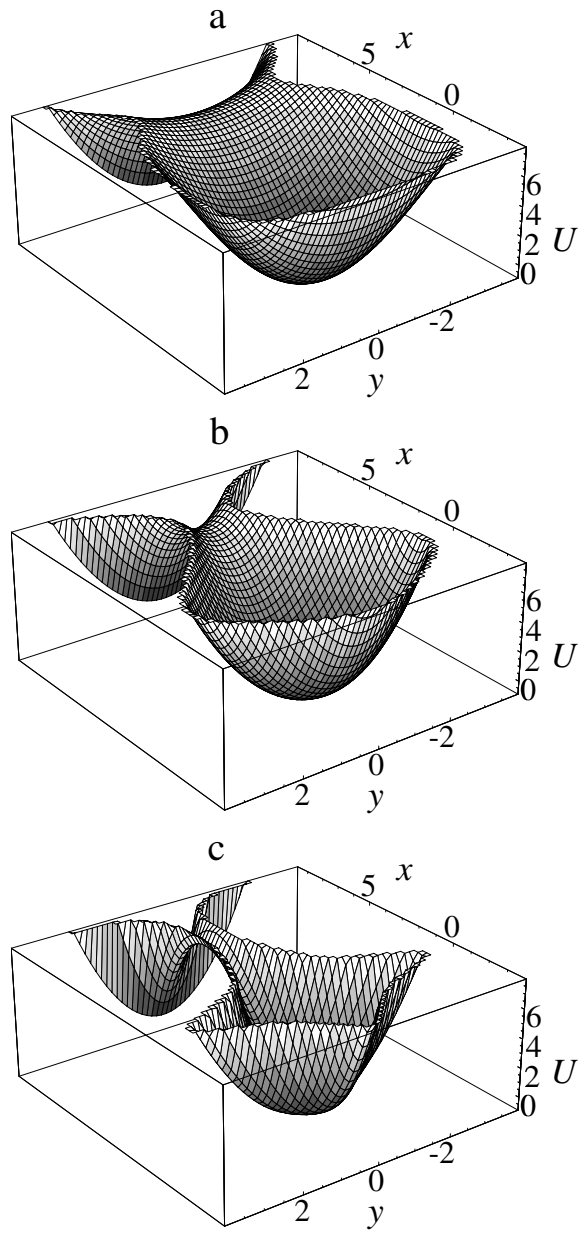


FIG. 2: The polynomial potential $U(x, y)$ of Eq. (5). We take $\hbar\omega_x$ as the basic energy units in this model. The other parameters are: $\omega_y = 1.7\omega_x$, $E_s = 7\hbar\omega_x$, with (a) $\omega_s = \omega_x$, (b) $\omega_s = 2.7\omega_x$, and (c) $\omega_s = 8\omega_x$.

allow for an analytic control of its shape through the adjustable parameters ω_x , ω_y , ω_s and E_s . Figure 2 depicts $U(x, y)$ for a few choices of these parameters. The origin is a local minimum, with harmonic frequencies ω_x and ω_y . A saddle point $(x_s, y_s) = (\sqrt{6E_s/\hbar\omega_x}, 0)$, of height E_s above the minimum, separates the stable region from the region of large positive x , where the potential has no lower bound. The quadratic expansion of the potential near the saddle point yields an imaginary frequency for

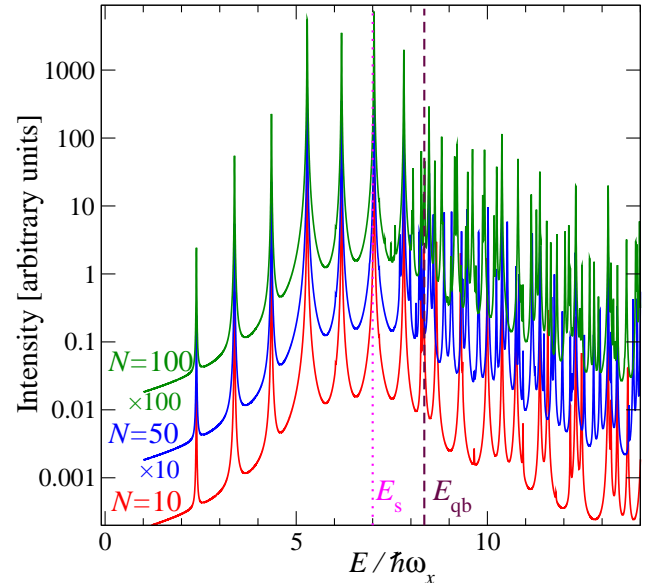


FIG. 3: The spectrum of the model of Eq. (5), parameters as in Fig. 2(b), initial state $|v_x=5, v_y=0\rangle$, and $\varepsilon=0.005\hbar\omega_x$. Bottom to top: $N=10$ (396 states), $N=50$ (7956 states), $N=100$ (30906 states). The sequence of converged peaks represents the v_x progression. Dense satellite lines (not converging with N) slightly below and above the quantum energy border (dashed line) E_{qb} indicate tunneling and leakage broadening.

the x motion $\omega'_x = i\omega_x$, and a harmonic one $\omega'_y = \omega_s$ for the surviving transverse mode. The y zero-point energy $E_{zp}^\perp = \hbar\omega_s/2$ extends the tunneling regime up to the quantum energy border $E_{qb} = E_s + \hbar\omega_s/2$. Sharp vibrational levels should therefore be found in the approximate range $(\hbar\omega_x + \hbar\omega_y)/2 \lesssim E \lesssim E_s + \hbar\omega_s/2$.

These expectations have been checked numerically by computing the eigenvalue spectrum. A standard way to evaluate the eigenvalues of an operator H is to compute the Green function

$$G(E + i\varepsilon) = \langle \mathbf{v}_0 | (E + i\varepsilon - H)^{-1} | \mathbf{v}_0 \rangle \quad (6)$$

for real E and a small positive imaginary part ε . The eigenvalues E_a of the exact eigenstates $|a\rangle$ of the Hamiltonian appear as poles in the complex plane slightly below the real axis. The reference state $|\mathbf{v}_0\rangle$ represents the initial excitation; for our model, Eq. (5), we take for $|\mathbf{v}_0\rangle$ an eigenstate $|v_x, v_y\rangle$ of the harmonic part of the Hamiltonian. The imaginary part of $-G(E + i\varepsilon)/\pi$ yields the lineshape function

$$I(E) = \frac{\varepsilon}{\pi} \sum_a \frac{|\langle a | \mathbf{v}_0 \rangle|^2}{(E - E_a)^2 + \varepsilon^2}. \quad (7)$$

Eigenvalues show up as peaks of $I(E)$, with heights proportional to the squared overlap of the exact eigenstates to the initial excitation. The parameter ε introduces an artificial Lorentzian broadening of the lines E_a .

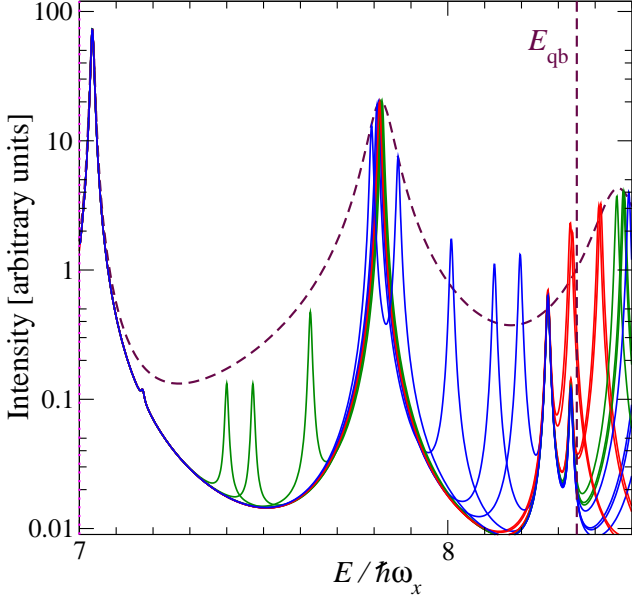


FIG. 4: A blowup of the spectrum of Fig. 3 in the region near E_{qb} , computed on bases with $N = 10, 11, \dots, 20$ tiers. The strongly basis-dependent satellites build up an envelope representative of tunneling and leakage broadening (dashed line). The envelope width of the state close to $7\hbar\omega$ is much smaller than the resolution $\varepsilon = 0.005\hbar\omega_x$ chosen for this calculation. The width of the next peak, at $7.8\hbar\omega$, is estimated $\Gamma \simeq 0.04\hbar\omega$; for the structures above E_{qb} , broadening becomes even larger, comparable to the inter-level separation.

The method for evaluating the Green function is non-perturbative, recursive, and it is applied in two steps. First, one constructs a basis of harmonic states grouped into families T_i (tiers), $i = 0 \dots N$, adapted to the specific PP and to the choice of the initial “bright” state $|\mathbf{v}_0\rangle$ (which constitutes tier T_0)^{23,24,25}. Next, the function $G(E + i\varepsilon)$ is evaluated through the exact recursive relation Eq. (A4), as detailed in the Appendix. Convergence of the spectrum against the basis size is tested by changing the single parameter N , the number of tiers. As the basis is finite, the spectrum consists of a finite number of real eigenvalues. Nevertheless, tunneling and leakage linewidth broadening shows in the comparison of spectra $I(E)$ of different tier number N . As we shall see, eigenvalues well below the quantum energy border E_{qb} correspond to stable sharp peaks. Near the border and in the leaking regime, evaluations with different N produce a number of weaker unphysical poles (not converging for increasing N) that decorate the resonant peaks.

Figure 3 reports the spectra computed for three largely different bases for the potential of Fig. 2(b) ($\omega_s = 2.7\hbar\omega_x$). Stable sharp levels of the v_x progression occur until slightly below the quantum border $E_{\text{qb}} = 8.35\hbar\omega_x$. Starting close to E_{qb} , dense non-converging satellites spring up, indicating a tunneling broadening exceeding the arbitrarily chosen spectral resolution $\varepsilon = 0.005\hbar\omega_x$. The proliferation of spurious peaks, which marks the on-

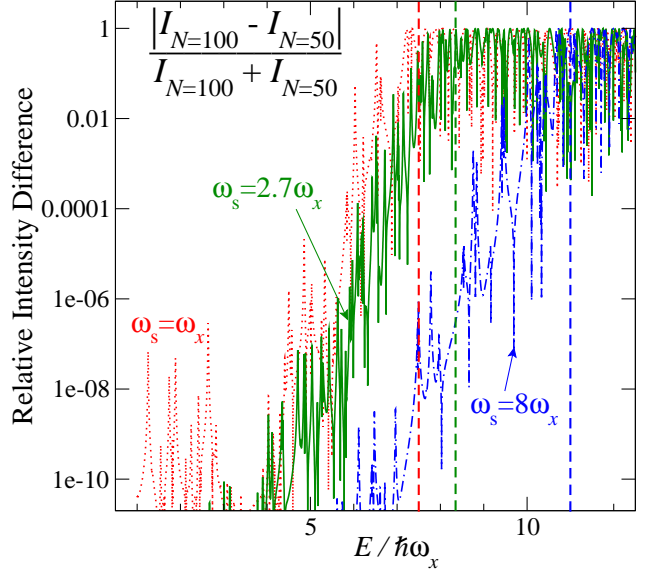


FIG. 5: The relative difference between the spectra of Fig. 3 computed on two very different bases ($N = 50$ and $N = 100$) as a function of energy for the three potentials of Fig. 2. The narrowing of the saddle valley – with associated increase in $E_{\text{qb}} = 7.5\hbar\omega_x, 8.35\hbar\omega_x$, and $11\hbar\omega_x$ (vertical dashed lines) – determines an enlargement of the region of convergence.

set of the leaking regime, is more manifest if one superposes several evaluations of $I(E)$ for different values of N . Figure 4 is a magnification of Fig. 3 in the crossover region near E_{qb} . The fitting envelope exhibits sharp peaks in the tunneling regime and substantial broadening in the leaking regime.

To better illustrate the role of $E_{\text{zp}}^\perp = \hbar\omega_s/2$, Fig. 5 plots the relative difference between the spectra computed on two different bases ($N = 50$ and $N = 100$) for the three potentials of Fig. 2. In the energy region of weak tunneling, this relative difference, associated to the weak satellite peaks representative of broadening, is extremely small, and it grows roughly exponentially with the energy distance to E_{qb} . Above E_{qb} , the relative difference is close to unity, indicating strong leakage. As expected, the region of weak tunneling enlarges with $\hbar\omega_s$, following the increasing E_{qb} .

We recall that the spectra of Fig. 3 and 5 correspond to an initial excitation given by the fourth ω_x overtone $|v_x = 5, v_y = 0\rangle$, a state with a substantial extension in the direction of the saddle. If a “transverse” initial excitation such as $|v_x = 0, v_y = 4\rangle$ is considered instead (see the spectrum in Fig. 6), tunneling is strongly suppressed, since the overlap of the initial excitation with the fast-leaking states is very small. Indeed, the main spectral structures are affected by much smaller broadening, even above the saddle, in comparison to the spectra of Figs. 3 and 6. This comparison exhibits a general feature of multidimensional PP ($d > 1$), namely the coexistence of weakly and strongly leaking states in the same energy range (above E_{qb}). For large d , the latter represent a

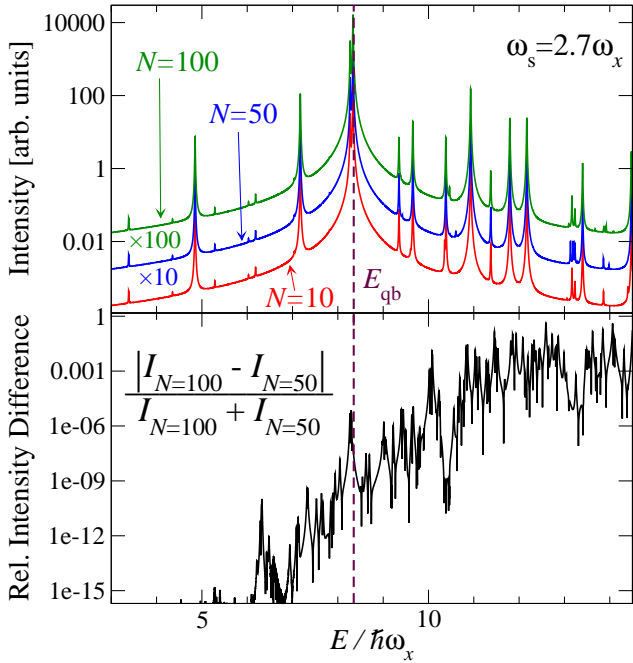


FIG. 6: Convergence of the spectrum as in Fig. 3, but for initial excitation $|v_x=0, v_y=4\rangle$ perpendicular to the direction of the saddle. Below E_{qb} (dashed line), and even above it, the main features are affected by much smaller broadening (few weak non-converging satellites, a substantially smaller relative difference in the lower panel) than with initial excitation $|v_x=5, v_y=0\rangle$ of Figs. 3-5.

minor fraction of all the states because of the small fraction of leaking directions over the whole solid angle in configuration space.

IV. A REAL MOLECULE: H_2O

As an illustration of the applicability of the tiers Green-function method to a real molecule and of the difficulties brought in by the energy border of the PP, we compute the vibrational spectrum of water. We employ the *ab-initio* quartic PP parameters listed in Table 6 of Ref. 5. The two real frequencies $\hbar\omega'_2 = 4758 \text{ cm}^{-1}$ and $\hbar\omega'_3 = 4849 \text{ cm}^{-1}$ at the lowest saddle point of H_2O ($E_s = 6846 \text{ cm}^{-1}$) are found so much larger than the three curvatures at the minimum, that $E_{\text{zp}}^{\perp} > E_{\text{zp}}(\mathbf{0})$ (Table I): this produces a rather narrow saddle, which pushes the quantum border up to $E_{\text{qb}} = 11649 \text{ cm}^{-1}$.

We take the harmonic fundamental excitation of the ω_1 (symmetric OH stretching) mode as initial state, and obtain the spectrum in Fig. 7. The peaks, representing exact vibrational levels, are assigned to the harmonic quantum numbers of the closest state resulting from standard second-order perturbation theory. Convergence is studied by increasing the tier number from $N = 5$ (not shown in figure) to $N = 10$ and 15: it is very good already using $N = 5$ tiers, thus showing the effectiveness

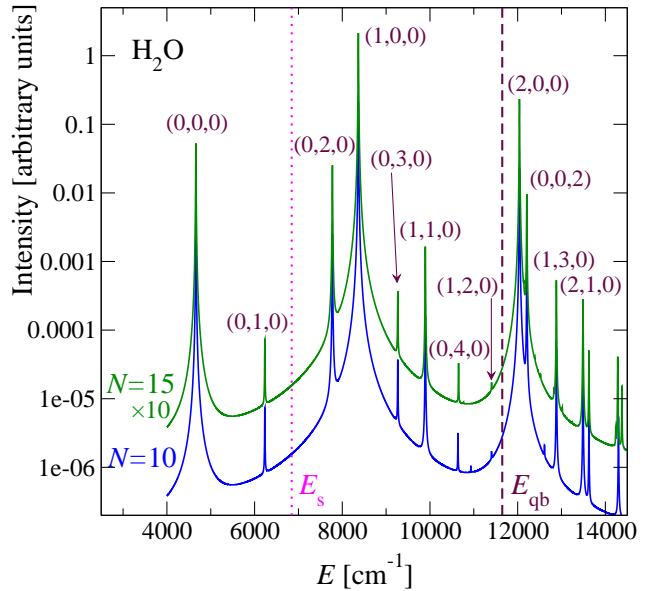


FIG. 7: The spectrum of H_2O for initial excitation $|v_1 = 1, v_2 = 0, v_3 = 0\rangle$, computed with $N=10$ (5570 states) and $N=15$ (16811 states), broadening $\varepsilon=4 \text{ cm}^{-1}$. Below the quantum energy border (dashed line) convergence is satisfactory with relative error $\leq 1\%$. Like in Fig. 6, the main features seem to converge also above E_{qb} , but the appearance of new structures for larger N indicates non-negligible leakage.

of the tiers Green-function method applied to a realistic problem. Like in the 2-dimensional model of Sec. III, hardly any tunneling is observed below E_{qb} . Across E_{qb} , the appearance of the weak non-converging satellites confirms that the resonances in this region are affected by significant leakage to the continuum. Indeed, since the lowest saddle lies in a direction involving mainly mode 1, the chosen initial state $|1, 0, 0\rangle$ encourages tunneling, like in the example of Fig. 3. Nonetheless, the stability of several features even above E_{qb} indicates that a number of fairly long-lived physical states are so localized in the well that their overlap to the outside continuum is relatively small. We are currently investigating a method to obtain an explicit evaluation of the tunneling widths Γ_a of the resonance states, by means of a complex coordinates transformation inspired by Ref. 19.

V. DISCUSSION

We show that, in general, polynomial approximations of molecular potentials display unphysical saddles that lead to regions where the potential is not lower-bounded. The height of the saddle and the zero-point energy of transverse modes both determine a quantum energy border.

In the spectral region below the quantum border, tunneling is exponentially small, the PP is reliable and standard perturbative treatment of the anharmonic interac-

tions usually provides a good approximation to the narrow level positions. Perturbative calculations are often extended to higher energies, based on the general belief that, like in the $d=1$ Morse case, the second-order approximation compensates the wrong behavior of the PP away from the minimum and reproduces the levels of a physical APES¹⁰.

Our non-perturbative calculations show that, as energy is raised above the quantum border, resonances leave the tunneling regime and couple more and more strongly to the continuum, practically washing out all spectral detail. Such highly excited states are of scarce physical relevance anyway, since the extension of the associated wavefunction explores regions where the PP becomes a very poor approximation of the true APES.

The present results cast a shadow on the traditional use of the polynomial approximation of the physical APES for the calculation of highly excited vibrational or roto-vibrational spectra of polyatomic molecules. For example, in most molecules, IVR (intramolecular vibrational relaxation) spectra involve energy levels much above the saddle. Hence, IVR applications of exact numerical methods, such as the Lanczos or Davidson algorithms^{26,27,28,29} or the Green-function method proposed here, are bound to face the problem of tunneling. The consequent broadening of the resonant states poses an intrinsic limit to the spectral accuracy which can be obtained. A real progress may be achieved by the use of smarter parametrizations of the APES (e.g. based on Morse coordinates), providing the correct large- \mathbf{Q} behavior.

APPENDIX A: NON-PERTURBATIVE EVALUATION OF THE GREEN FUNCTION.

We present a general procedure, inspired to Ref. 30 and there indicated as “tiers method”, for the non-perturbative evaluation of the eigenvalues and spectral weights of a Hamiltonian decomposed as $H = H_0 + V$. It is assumed that the eigenvectors of H_0 are well characterized and that the matrix elements of V are easy to compute and link any eigenstate of H_0 with a finite (not too large) number of other eigenstates. For definiteness, we consider the problem at hand of the vibrational levels in a polynomial potential (2). The term $H_0 = \sum \hbar\omega_i(a_i^\dagger a_i + 1/2)$ describes d independent oscillators, with eigenvectors $|\mathbf{v}\rangle = |v_1, v_2, \dots, v_d\rangle$ that specify the occupation numbers of the d oscillators. V is the anharmonic part of the potential, V^{anhar} .

The first step of the method is to partition the unperturbed eigenvectors in families (tiers), T_0, T_1, \dots of decreasing perturbative relevance. The construction is such that the matrix representation of H is block-tridiagonal in the tiers. Symbolically we write the blocks as $H_{ii} = \langle T_i | H | T_i \rangle$ and $H_{i,i+1} = \langle T_i | H | T_{i+1} \rangle$.

Next, we provide an exact iteration scheme for the evaluation of the matrix elements of the resolvent $G(z) =$

$(zI - H)^{-1}$ in the basis vectors $|\mathbf{v}_{0,\alpha}\rangle$ in Tier 0. The poles give the eigenvalues E_a of H , and the residues are the spectral weights:

$$G^{(0)}(z)_{\alpha,\beta} = \sum_a \frac{\langle \mathbf{v}_{0,\alpha} | E_a \rangle \langle E_a | \mathbf{v}_{0,\beta} \rangle}{z - E_a} \quad (\text{A1})$$

The actual evaluation requires approximations such as truncation of the tier generation to some order, and possibly restriction of tier population. Anyhow, as the method is iterative and in analogy with procedures that approximate a self-energy, the resulting matrix elements of $G^{(0)}(z)$ are highly non-perturbative.

Tier construction

Depending on the problem under investigation, a set of t_0 unperturbed states $|\mathbf{v}_{0,\alpha}\rangle$ ($\alpha = 1, \dots, t_0$) is selected to form the initial tier T_0 . In the computations of this paper, T_0 contains a single state, the bright state. The action of V on T_0 gives new vectors; the basis states that have non-zero overlap with one of them, and are not in T_0 , are collected in T_1 . We label them as $|\mathbf{v}_{1,\alpha}\rangle$ ($\alpha = 1 \dots t_1$). For a finite set T_0 , and an interaction V which is a polynomial in the raising and lowering operators, tier T_1 and subsequent ones are finite.

Next we consider the set VT_1 , and expand it in the eigenvectors already in T_0 and T_1 , plus new ones that are collected in tier T_2 . The process is iterated to produce further tiers T_3, T_4, \dots . Up to this point the method is simply a smart algorithm to generate systematically a good approximate basis for a quantum problem where some non-interacting part H_0 of the Hamiltonian can be singled out. Indeed, such a basis has been employed successfully in a different context, in conjunction with standard (Lanczos) techniques.³¹ However, the hierarchical basis structure and the corresponding block-tridiagonal form of the Hamiltonian, suggest a natural iterative method to construct the spectrum.

Evaluation of the Resolvent

The iterative method is based on the following formula for the inversion of partitioned matrices, with square diagonal blocks (we omit unneeded terms):

$$M = \begin{pmatrix} M_{11} & M_{12} \\ M_{21} & M_{22} \end{pmatrix}$$

$$M^{-1} = \begin{pmatrix} [M_{11} - M_{12}(M_{22})^{-1}M_{21}]^{-1} & \dots \\ \dots & \dots \end{pmatrix} \quad (\text{A2})$$

We apply this formula by identifying M with the matrix representations of $zI - H = (zI - H_0) - V$ and M^{-1} with $G(z)$. The blocks result from the separation of the basis into the set T_0 and the ordered set $T_1 \cup T_2 \cup \dots$ In this tier basis, off-diagonal matrix elements of M only arise from the action of V . Thus $M_{11} = zI_0 - H_{00}$ (I_0 is the unit matrix of size t_0 and $H_{00} = \langle T_0 | H | T_0 \rangle$). M_{22} is the matrix $(zI - H)$ expanded in the remaining tiers. $M_{12} = M_{21}^t$ is a rectangular matrix of size $t_0 \times (t_1 + t_2 + \dots)$; by the tier construction, non-zero matrix elements of the

potential are only in the leftmost submatrix of size $t_0 \times t_1$, that identifies with the matrix $-V_{01} = -\langle T_0 | V | T_1 \rangle$.

The aim of the calculation is to evaluate the block $(M^{-1})_{11} \equiv G^{(0)}(z)$, Eq. (A1). The inversion formula (A2) provides

$$\begin{aligned} G^{(0)}(z) &= [M_{11} - M_{12}(M_{22})^{-1}M_{21}]^{-1} \\ &= [zI_0 - H_{00} - V_{01}G^{(1)}(z)V_{10}]^{-1} \end{aligned} \quad (\text{A3})$$

We defined the $t_1 \times t_1$ matrix $G^{(1)}(z) = \langle T_1 | (M_{22})^{-1} | T_1 \rangle$. To evaluate it we use Eq. (A2) again, with the blocks now resulting from the separation of the basis into the set T_1 and the set $T_2 \cup T_3 \cup \dots$. Now the block M_{11} is $(zI_1 - H_{11})$ and M_{22} is the matrix $(zI - H)$ expanded in the basis $T_2 \cup T_3 \cup \dots$. The matrix $G^{(1)}(z)$ coincides with the block $(M^{-1})_{11}$. The formula (A2) provides:

$$G^{(1)}(z) = [zI_1 - H_{11} - V_{12}G^{(2)}(z)V_{21}]^{-1}$$

where $G^{(2)}(z) = \langle T_2 | (M_{22})^{-1} | T_2 \rangle$. By iterating the same inversion formula (A2) we obtain a chain of relations of the type

$$G^{(k-1)}(z) = [zI_{k-1} - H_{k-1,k-1} - V_{k-1,k}G^{(k)}(z)V_{k,k-1}]^{-1} \quad (\text{A4})$$

In practice, the (in principle infinite) chain is truncated by approximately taking $G^{(N)}(z) \approx (zI_N - H_{NN})^{-1}$. This assumption is in order if the coupling of T_N to the subsequent tier is negligible. Starting from $G^{(N)}(z)$, one iterates (A4) back to the sought for matrix $G^{(0)}(z)$. This procedure is a matrix generalization of the continued fraction expansion for the inversion of tridiagonal matrices.³²

Discussion

The method just outlined generates an effective basis and solves the quantum mechanical problem in the reduced Hilbert space exactly. The basis can be enlarged systematically by increasing the number of tiers N , to achieve

convergence. When applied to a lower-bounded PP, this method provides an efficient and rapidly converging numerical scheme to determine its exact eigenenergies. For the lower-unbound PP of a polyatomic molecule, this method provides good estimates of the position of the quasi-stationary states, including a rigorous treatment of all anharmonic resonances. The recursive calculation of the Green's function (A4) has several advantages with respect to the more traditional Lanczos method:^{27,31,33,34} (i) it provides equal accuracy through the whole spectrum, while Lanczos method is more accurate close to the endpoints; (ii) it splits the Hilbert space into subspaces T_0, \dots, T_N to treat one at a time; (iii) once the chain of matrices is set up, each frequency requires an independent calculation, which makes this method suitable for parallel calculations. Its main disadvantage is the rapid growth of the tier size t_i , for systems with many degrees of freedom. To fit the available CPU/memory limits, it is possible to cutoff the tier growth to some maximum size t_{\max} , as described in Ref. 31. In general, the recursive method may become very costly in CPU time, since the evaluation of $G^{(0)}(E + i\varepsilon)$ requires N inversions for each sample frequency E , each inversion costing a time proportional to t_{\max}^3 . In the Lanczos method, a single chain of $N_{\text{Lanczos}} \approx 10^3$ iterations, each costing of the order of the Hilbert space size $\sim N \cdot t_{\max}$, generates the whole spectrum.

The c++ code for computing the tier basis and the spectrum based on the Green-function recursive inversion formula (A4) is available in Ref. 35.

ACKNOWLEDGEMENTS

We thank J.H. van der Waals, G. Scoles, K. Lehmann, and A. Callegari for useful discussions.

* Electronic address: nicola.manini@mi.infn.it

† Electronic address: luca.molinari@mi.infn.it

‡ Electronic address: gian.paolo.brivio@mater.unimib.it

¹ M. N. Ramquet, G. Dive and D. Dehareng, *J. Chem. Phys.* **112**, 4923 (2000).

² *Global and Accurate Vibration Hamiltonians from High-Resolution Molecular Spectroscopy*, edited by M. Herman, J. Lievin, J. W. Auwera and A. Campargue, *Adv. in Chem. Phys.* vol. **108** (Wiley, New York 1999).

³ E. Bright Wilson, J. C. Decius, and P. C. Cross, *Molecular Vibrations, The Theory of Infrared and Raman Vibrational Spectra* (McGraw-Hill, New York, 1955).

⁴ *Ab initio and ab initio derived force fields: state of the science*, editor T. J. Lee, *Spectrochim. Acta A* **53**, Special Issue (1997).

⁵ A. G. Császár and I. M. Mills, *Spectrochim. Acta A* **53**, 1101 (1997).

⁶ J. M. L. Martin, T. J. Lee, P. R. Taylor, and J. P. François,

J. Chem. Phys. **103**, 2589 (1995).

⁷ A. Miani, E. Cane, P. Palmieri, A. Trombetti, and N. C. Handy *J. Chem. Phys.* **112**, 248 (2000).

⁸ R. Burcl, N. C. Handy, and S. Carter, *Spectrochim. Acta A*, **59**, 1881 (2003).

⁹ J. Demaison, A. Perrin, and H. Burger, *J. Mol. Spectr.* **221**, 47 (2003).

¹⁰ I. M. Mills and A. G. Robiette, *Mol. Phys.* **56**, 743 (1985).

¹¹ P. Hänggi, P. Talkner, and M. Borkovec, *Rev. Mod. Phys.* **62**, 251 (1990).

¹² B. H. Bransden and C. J. Joachain, *Physics of Atoms and Molecules* (Prentice Hall, Englewood Cliffs, NJ, 2003).

¹³ J. Koput and K. A. Peterson, *Chem. Phys. Lett.* **283**, 139 (1998).

¹⁴ A. East, W. Allen, and S. Klippenstein, *J. Chem. Phys.* **102**, 8506 (1995).

¹⁵ A. Miani, V. Hänninen, M. Horn, and L. Halonen, *Mol. Phys.* **98**, 1737 (2000).

¹⁶ V. A. Benderskii, D. E. Makarov, and C. A. Wight, *Chemical Dynamics at low temperatures*, Adv. Chem. Phys. vol. **88**, (Wiley, New York 1994).

¹⁷ P. Hanggi, U. Weiss, and P. Riseborough, Phys. Rev. A **34**, 4558 (1986).

¹⁸ J. Zamastil, V. Špirko, J. Čížek, L. Skála, and O. Bludský Phys. Rev. A **64**, 042101 (2001).

¹⁹ R. Yaris, J. Bendler, R. A. Lovett, C. M. Bender, and P. A. Fedders, Phys. Rev. A **18**, 1816 (1978).

²⁰ G. Alvarez, Phys. Rev. A **37**, 4079 (1988).

²¹ T. N. Rescigno, M. Baertschy, D. Byrum, and C. W. McCurdy, Phys. Rev. A **55**, 4253 (1997).

²² H. Kitamura, S. Tsuneyuki, T. Ogitsu, and T. Miyake, Nature **404**, 259 (2000).

²³ M. Bixon and J. Jortner, J. Chem. Phys. **48**, 715 (1968).

²⁴ T. Uzer, Phys. Rep. **199**, 73 (1991).

²⁵ K. T. Marshall and J. S. Hutchinson, J. Chem. Phys. **95**, 3232 (1991).

²⁶ M. Gruebele, J. Chem. Phys. **104**, 2453 (1996).

²⁷ R. Wyatt, J. Chem. Phys. **109**, 10732 (1998).

²⁸ J. Pochert, M. Quack, J. Stohner, and M. Willeke, J. Chem. Phys. **113**, 2719 (2000).

²⁹ A. Callegari, R. Pearman, S. Choi, P. Engels, H. Srivastava, M. Gruebele, K. K. Lehmann, and G. Scoles, Mol. Phys. **101**, 551 (2003).

³⁰ A. A. Stuchebrukhov and R. A. Marcus, J. Chem. Phys. **98**, 6044 (1993).

³¹ N. Manini, P. Gattari, and E. Tosatti, Phys. Rev. Lett. **91**, 196402 (2003).

³² R. Haydock, *The recursive solution of the Schrödinger equation*, Solid State Physics Vol. 35 (Academic Press, New York, 1980).

³³ J. Jaklic and P. Prelovsek, Adv. Phys. **49**, 1 (2000).

³⁴ H. Köppel, M. Döscher, I. Bâldea, H.-D. Meyer, and P. G. Szalay, J. Chem. Phys. **117**, 2657 (2002).

³⁵ A. Del Monte and N. Manini, <http://www.mi.infm.it/manini/ivr.html>.

³⁶ For example, the fourth-order terms $\Phi_{1111}Q_1^4 + \Phi_{1222}Q_1Q_2^3 + \Phi_{2222}Q_2^4$ combine to $(\gamma^4\Phi_{1111} + \gamma\Phi_{1222} + \Phi_{2222})Q_2^4$ along the line $Q_1 = \gamma Q_2$, and the numeric coefficient $\gamma^4\Phi_{1111} + \gamma\Phi_{1222} + \Phi_{2222}$ can easily be negative, provided that $|\Phi_{1222}|$ is large enough and that γ is chosen suitably. Also, to make things worse, even though fully diagonal Φ_{aaaa} terms are usually positive, there often occur semi-diagonal terms Φ_{aabb} with negative sign.